Fermilab FERMILAB-TM-2160 November 2001

Fermi National Accelerator Laboratory

Fermilab-TM-2160
September 28, 2001

Cost optimization of a hadron collider

Vadim V. Kashikhin, Peter J. Limon

Fermilab, P.O. Box 500, Batavia, IL 60510

2001

Operated by Fermi Research Alliance, LLC under Contract No. DE-AC02-07CH11359 with the United States Department of Energy.

Abstract

This paper discusses cost scaling laws and optimization of hadron colliders based on high field magnets. Using a few simplifying assumptions that should give a reasonable approximation, cost of the magnet is divided among several major components. Scaling law for every component is determined along with the weight factors that allow cost comparison between different magnet designs. Cost of hadron collider as a function of field, aperture size and critical current density in superconductor is described analytically that allows cost optimization by changing magnet parameters. The optimum magnetic field is determined for machines based on NbTi superconductor, operating at 4.2 K or 1.9 K and Nb_3Sn superconductor operating at 4.2 K. Analyzed influence of main magnet design parameters on a machine cost provided information on ways leading to the magnet cost reduction. Economical justification of a Nb_3Sn collider is performed, which lets to determine the maximum price ratio between Nb_3Sn and NbTi superconductors that makes Nb_3Sn collider economically effective.

1. Optimization of the coil area

Simulation of the coil configuration, required for generation of uniform dipole field *B* within aperture of a given radius *r*, in many cases involves numerical optimization of multiple conductor positions around the aperture. A theoretical limit for optimum coil configuration (with minimum cross-section area and cost) can be, however, derived semi-analytically.

Let us find a coil configuration based on two intersecting ellipses that generates uniform magnetic field with the flux density *B* inside aperture with radius *r* (Figure 1) and has a minimum possible cross-section area. The current-carrying superconducting material is assumed to have critical current density J_c at the field B_0 and some temperature, while being uniformly distributed together with copper stabilizer within the ellipses.

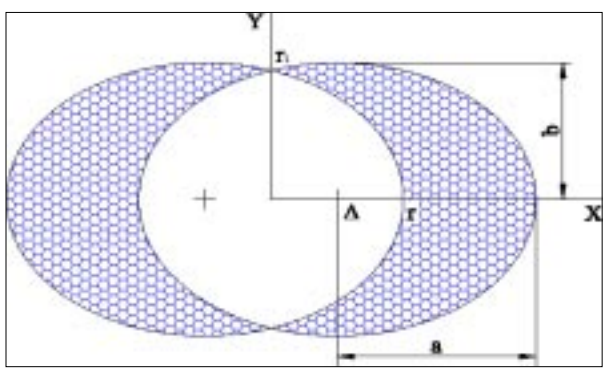

Figure 1. Naming convention for the idealized coil parameters.

Copper to non-copper ratio[1] is also uniform and equals K_{cusc}. The critical current density of Nb_3Sn superconductor can be expressed as a function of applied field *B* according to [1]:

$$J_c(B) = \frac{C}{\sqrt{B}}\left(1 - \frac{B}{B_{c2}}\right)^2,$$

[1] Under this term here and after we understand ratio between non-superconducting and superconducting parts.

where B_{c2} is the upper critical field of superconductor and C is constant defined as:

$$C = \frac{J_c(B_0)\sqrt{B_0}}{\left(1-\frac{B_0}{B_{c2}}\right)^2}.$$

The dependence is virtually linear for NbTi superconductor, thus can be expressed by:

$$J_c(B) = C_1 - B \cdot C_2,$$

where C_1 is determined by operating temperature and C_2 is constant.

The effective (mean) current density in a conductor containing copper and superconductor fractions is:

$$J(B) = \frac{J_c(B)}{1+K_{cusc}}.$$

Cross-section area of two ellipses with taken out region of intersection can be written as:

$$S = 2\left\{\pi ab - 2\left[ab \cdot \arccos\left(\frac{\Delta}{a}\right) - \Delta r_1\right]\right\}. \tag{1.1}$$

The y-position of intersection point of two ellipses can be derived from the ellipse equation:

$$r_1 = b\sqrt{1-\left(\frac{\Delta}{a}\right)^2} \tag{1.2}$$

The field generated by two elliptical conductors is uniform within area of intersection and equals:

$$B = 2\mu_0 J_c(B)\frac{b\Delta}{a+b}. \tag{1.3}$$

As most of the accelerator magnets should have circular aperture by technological reasons, one need to apply constrains for fitting a circle with radius r inside the aperture. A distance from the origin of coordinates to a point on the ellipse with coordinate x is determined as:

$$r_b(x) = \sqrt{x^2+y^2} = \sqrt{x^2 + b^2\left(1-\frac{(x-\Delta)^2}{a^2}\right)} \tag{1.4}$$

Taking a derivative one can find x that correspond to a minimum $r_b(x)$ from equation:

$$\frac{dr_b(x)}{dx} = 0,$$

that equals to:

$$x_{\min} = \frac{b^2\Delta}{b^2-a^2}. \tag{1.5}$$

Therefore the constrain needed to be satisfied for the circle with radius r to fit inside the coil aperture is:

$$r_b(x_{\min}) \to r$$

Now one has determined all the necessary expressions to find the coil geometry for a given set of parameters. Combining (1.1) -(1.5) into three equations one can define a system to be solved:

$$\begin{cases} 2\left\{\pi ab - 2b\left[a \cdot a\cos\left(\frac{\Delta}{a}\right) - \Delta\sqrt{1-\frac{\Delta^2}{a^2}}\right]\right\} = S \\ 2\mu_0 J(B) b \frac{\Delta}{a+b} = B \\ b\sqrt{\left(\frac{b\Delta}{b^2-a^2}\right)^2 - \frac{1}{a^2}\left(\frac{b^2\Delta}{b^2-a^2} - \Delta\right)^2 + 1} = r \end{cases} . \tag{1.6}$$

The number of unknown variables in the system exceeds number of equation, meaning that there are multiple sets of variables, simultaneously satisfying the system. However, there is only one set of variables for every aperture size, field and critical current density that correspond to the minimum coil area. It was found using the Levenberg-Marquardt's optimization method implemented in MathCad program package under condition $S \to 0$.

2. Magnet cost scaling laws

In order to perform cost analysis and optimization of a collider one should determine major cost drivers and their scale laws. The magnet cost can be virtually divided between three major contributors: coil, cold mass and cryostat. Since lengths of high field magnets are usually much bigger than their transverse size, the magnet cost per unit of length can be assumed to be proportional to the sum of cross-section areas of these three components with relevant cost factors:

$$C'_{mag} = S_{coil}K_{coil} + S_{cm}K_{cm} + S_{cr}K_{cr} \tag{2.1}$$

Scaling law for the coil area has been determined in previous paragraph. The yoke and skin drive cross-section area and cost of the cold mass. Assuming equal yoke saturation and fringe field as the scaling criteria for yoke size, one can say that ratio of magnetic flux, generated by the coil to the yoke outer radius should remains constant:

$$R_{yoke} \sim R_{bore}B$$

or

$$S_{yoke} \sim R_{bore}{}^2 B^2 \tag{2.2}$$

It leads to approximately constant flux density, yoke saturation and fringe field, for yokes with relatively big radii ("cold" yoke magnets).

Scaling criteria for the skin thickness is the constant tensile stress created in skin by electromagnetic forces. Horizontal force per unit of coil shell length is proportional to:

$$F'_x \sim B_y I_z$$

or

$$F' \sim B^2$$

for a fixed bore radius. Variations in the bore radius would require proportional adjustment of current in the coil in order to maintain a constant field. Therefore in general, the force depends on the field and bore radius as:

$$F' \sim R_{bore} B^2 .$$

Now one can find scaling law for the skin area. Equality of tensile stresses imposes keeping a constant ratio between force F' and skin thickness d_{skin} that means:

$$d_{skin} \sim F' \sim R_{bore} B^2$$

Since the skin area is proportional to the skin (yoke) radius R_{yoke} times skin thickness d_{skin} we can write the final dependence:

$$S_{skin} \sim R_{bore} d_{skin} \sim R_{bore}{}^2 B^3 . \tag{2.3}$$

Comparing (2.2) and (2.3) one can see that skin area grows faster than yoke area by a power of B. For simplicity we can assume that the extra force is taken by some slim collar around the coil and the cold mass area scales as:

$$S_{cm} \sim S_{skin} + S_{yoke} \sim R_{bore}{}^2 B^2 .$$

The cryostat area is proportional to its radius times thickness. Since the thickness virtually does not depend on the parameters of the magnet it houses, we can write:

$$S_{cr} \sim R_{yoke} + \Delta R ,$$

where ΔR is the radial space between cryostat and iron yoke. For simplicity this space can be assumed to be proportional to the yoke radius, then:

$$S_{cr} \sim R_{bore} B .$$

We have now determined all necessary laws to scale magnet cost for any field and bore radius:

$$C'_{mag}(R_{bore}, B) \sim S_{coil}(R_{bore}, B) K_{coil} + R_{bore}{}^2 B^2 K_{cm} + R_{bore} B K_{cr} . \tag{2.4}$$

In order to find the cost factors one should use some reference magnet with known contribution of magnet components into the total magnet cost. RHIC dipole magnet is used for this purpose as is has typical for high field magnets design and parameters. Table 2.1 presents cost distribution between the main magnet components [2].

Table 1. Cost distribution of RHIC dipole magnet.

Component	**Materials, %**	**Labor, %**	**Total, %**
Total	**62**	**38**	**100**
Coil	18	11	29
Cold mass	21	13	34
Cryostat	23	14	37

One can see that the labor part makes a considerable contribution into the magnet cost. However it is difficult to establish direct scaling laws for the labor part as it is not obviously related to magnet parameters, like field and aperture size, but rather to types of materials and technological procedures used during magnet fabrication. For simplicity we can assume that the labor part scales directly proportional to the materials part (which should be true for relatively large orders).

Taking cost of the RHIC dipole magnet for 1 unit of relative magnet cost we can determine the cost factors. Solving system (1.6) for the specific RHIC parameters: B = 3.46 T, R_{bore} = 4 cm, NbTi superconductor with C_1 = 6000 A/mm^2, C_2 = 600 A/mm^2/T and K_{cusc} = 2.2 one finds the coil area S_{coil} = 7.47 cm^2. This value is smaller than the actual area of the RHIC coil since it assumes the ideal coil configuration without spacers between coil blocks and no margin in the bore field. Keeping it the same way for any other magnet with different field and bore radius would assure that the magnet has the same packing factor of cables in the coil and bore field margin (15 %) as the RHIC dipole. Table 2 presents cost factors that satisfy (2.4) for the RHIC dipole parameters.

Table 2. Cost factors.

Component	**Cost factor**	**Scaling law**
Coil	$3.88\cdot10^{-2}$ 1/cm^2	S_{coil}
Cold mass	$1.77\cdot10^{-3}$ 1/T^2/cm^2	$R_{bore}{}^2B^2$
Cryostat	$2.67\cdot10^{-2}$ 1/T/cm	$R_{bore}B$

Note that the scale factors represent relative cost of the material and irrelevant to magnet design or parameters, which allows to estimate cost of any other high field magnet using determined scale laws in the units of the RHIC magnet cost per unit of length. Figure 2 shows relative cost of high field magnet based on the NbTi coils, operating at 4.2 K (RHIC parameters) or 1.9 K temperature (with C_1 = 7800 A/mm^2, C_2 = 600 A/mm^2/T) and Nb_3Sn coil operating at 4.2 K (B_{c2} = 24.88 T, J_c(12 T) = 3000 A/mm^2).

The copper to non-copper ratio in the coils was 0.85, which is safe minimum required for the micro-quench stabilization. Necessary for the quench protection amount of copper can be introduced using the sub-strand approach [3], which does increase the coil area but virtually does not contribute to the coil cost and generally leads to 15-20 % cost reduction of the superconducting cable. The coil bore diameter was set to 40 mm, proven to be reliable by recent VLHC Design Study [4]. The plot also shows relative magnet cost curves for SSC and LHC machines.

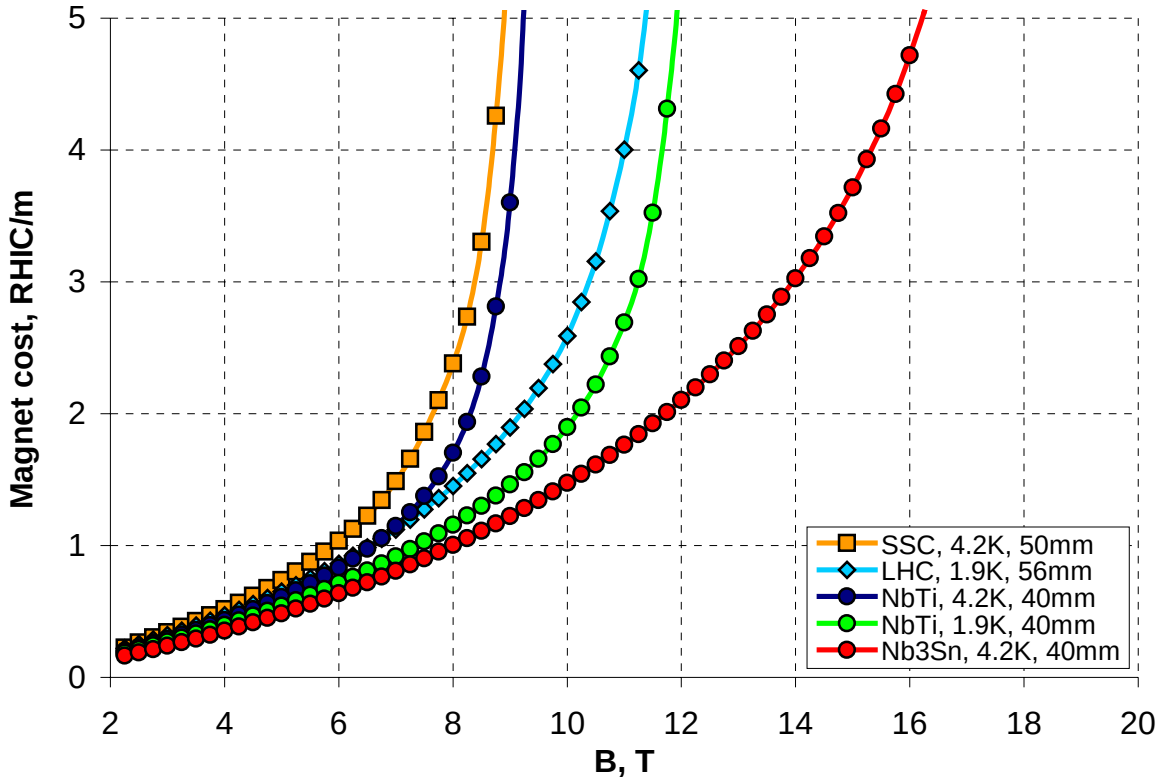

Figure 2. Magnet cost as a function of field.

3. Collider cost

Similarly to the scaling expression for the magnet cost, we can define a collider cost function as:

$$C_{col} = C'_{mag} \cdot L + C'_{tun} \cdot L + C_{const} ,$$

where L is the collider circumference, C_{mag}' is the cost of magnets per unit of length, C_{tun}' is the tunnel, instrumentation and cryogenics cost per unit of length and C_{const} are some constant expenses, irrelevant to the machine parameters. It is convenient to compare costs of fully equipped tunnels in units per T·m or TeV. Since the constant expenses are not consistent with such representation, they were subtracted from the equation:

$$C'_{eqtun} \sim \frac{1}{B}\left(C'_{mag} K_{mag} + C'_{tun} K_{tun}\right).$$

In order to determine the cost factors one can use cost distribution for some reference machine, similarly to the magnet case. Table 3 presents the cost distribution for the SSC project, escalated to FY2001 dollars [5].

The ratio between magnet and non-magnet part in this table is 56 % over 44 %. Since the cost ratio is given for the double beam machine – the scaling will be correct for a double beam machine only. One also needs to calculate the coil area for the SSC magnet parameters: B = 6.8 T, R_{bore} = 2.5 cm, NbTi superconductor with C_1 = 6000 A/mm^2, C_2 = 600 A/mm^2/T and K_{cusc} = 1.6. The coil area corresponding to these parameters is S_{coil} = 17.73 cm^2.

Table 3. Cost distribution of SSC project.

Component	FY2001, K$	Ratio
Total	**3,651,187**	**100.00%**
Civil Underground	558,160	15.29%
Civil Above Ground	170,133	4.66%
Arc Magnets	2,043,811	55.98%
Correctors & Special Magnets	168,622	4.62%
Vacuum	17,341	0.47%
Installation	121,487	3.33%
Cryogenics	266,828	7.31%
Interaction Regions	87,133	2.39%
Other Accelerator Systems	217,672	5.96%

If to take cost of building 1 m of fully equipped SSC tunnel for 1 unit we can find the cost factors: K_{mag} = 2.76 T and K_{tun} = 2.99 T. Figure 3 shows cost of the fully equipped tunnel per T·m for three choices of superconductors, considered in previous paragraph. Dividing total cost of the fully equipped SSC tunnel by the operating field of 6.8 T and the machine circumference of 87 km one finds the SSC collider cost of 6172 $/T/m, which makes it possible to plot the cost distribution in absolute units (Figure 4).

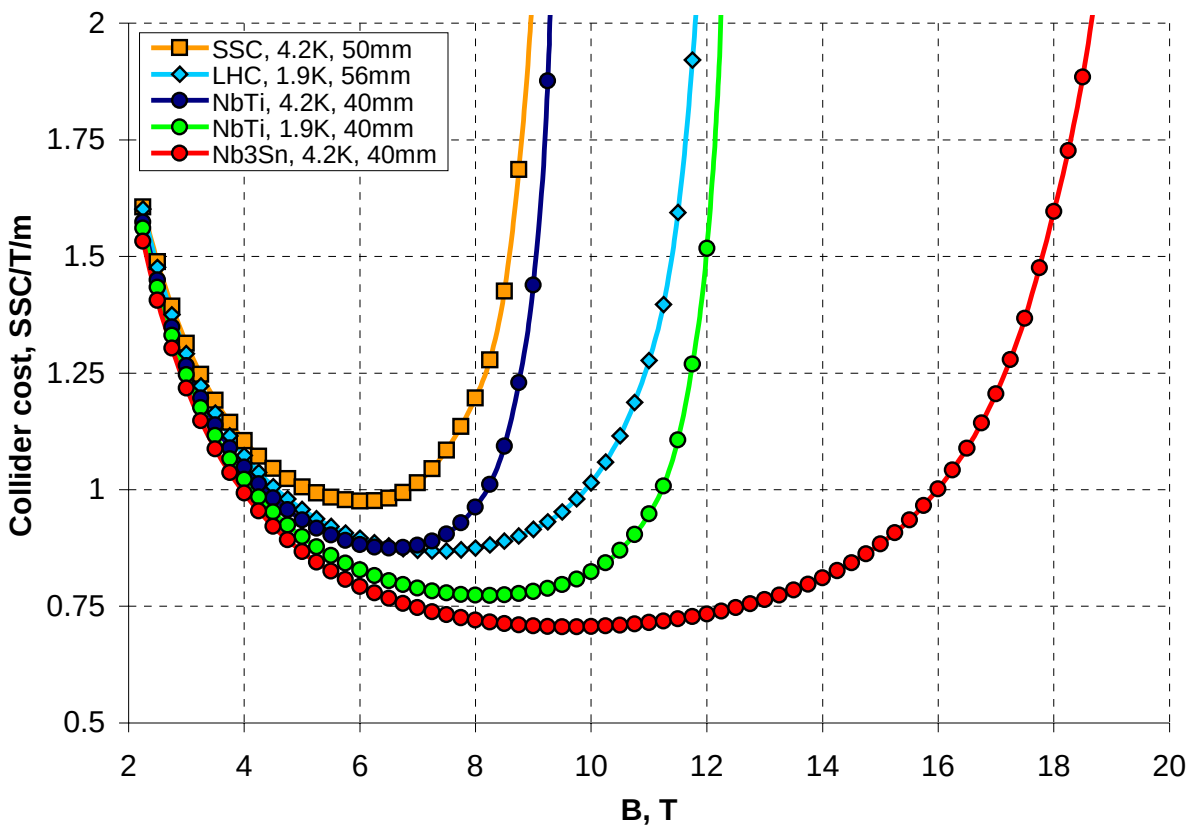

Figure 3. Collider cost as a function of field in SSC units.

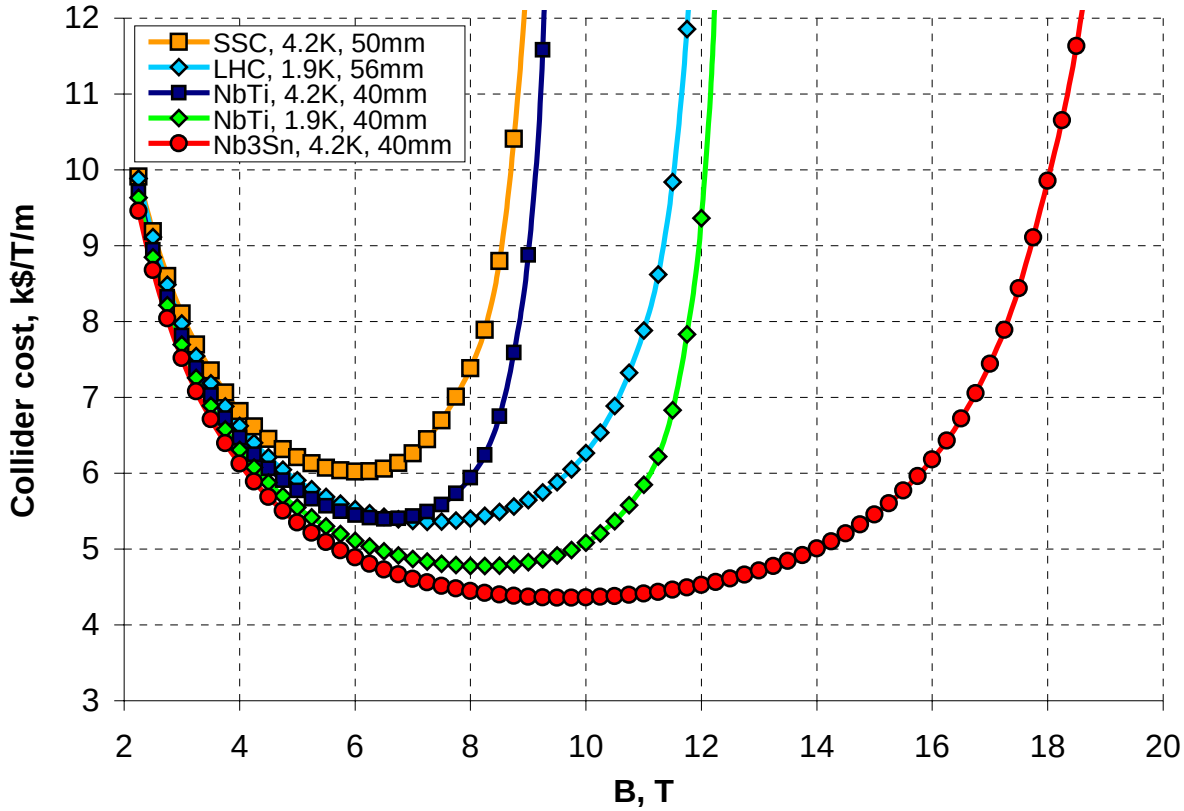

Figure 4. Collider cost as a function of field in FY2001 dollars.

4. Analysis of the magnet design parameters

Results of the previous paragraph demonstrated cost dependencies for machines with different superconductor properties and aperture sizes. It is interesting to separately analyze effect of each particular parameter on the machine cost and optimum field. For this purpose the critical current density in superconductor was fixed at J_c(12 T, 4.2 K) = 3000 A/mm^2, copper to non-copper ratio in the coil at 0.85 and coil bore diameter was consequently varied within 30-50 mm with 5 mm increment. Figure 5 shows collider cost as a function of field for different bore diameters and Figure 6 derives minimum cost and optimum field as functions of bore diameter. One can notice that decreasing of the coil bore diameter from the "proven-to-be-feasible" 40 mm to somewhat "close-to-the-limit" 30 mm (or by 33 %) leads to decreasing of the collider cost by only 2 %. However, inevitable growth of the beam screen, cryogenics and magnet alignment system cost (not included in this model), may very likely make smaller aperture option more expensive. In fact, larger than 40 mm aperture may turn out to be more cost effective, especially for higher than 10 T field magnets, when synchrotron radiation starts playing a significant role in magnet design. The optimum field depends nearly inversely proportional to the bore diameter and changes from 9.64 T to 9.9 T for the 40 mm to 30 mm aperture change.

Influence of the second parameter – critical current density was analyzed for the coil bore diameter fixed at 40 mm and copper to non-copper ratio in the coil of 0.85. Figure 7 shows collider cost as a function of field for different critical current densities in superconductor at

12 T and 4.2 K and Figure 8 derives minimum cost and optimum field as functions of critical current density. It is interesting to notice that the collider cost and optimum field changes significantly within the range of 1000-3000 A/mm^2 and starts to "saturate" for higher values. Thus the cost drops by 16 % for the first 2000 A/mm^2 and only by 4 % for the second one. It explains by the fact that the coil area and therefore its contribution to the cost decrease at a higher critical current density, when the rest of components contribute nearly constant amount. Obviously, reaching of higher critical current densities requires additional investments to the technology (at least at the R&D stage) that reduces benefits of such conductors even more.

The last parameter necessary to analyze was the copper to non-copper ratio. Since it is in direct correlation with the current density in superconductor, a new copper to non-copper ratio can be calculated as:

$$K_{cusc}^{new} = \frac{J_c^{new}}{J_c^{old}}\left(1 + K_{cusc}^{old}\right) - 1,$$

under assumption that current in the coil remains constant. Having fixed the critical current density at 3000 A/mm^2, it is easy to derive minimum collider cost and optimum field as functions of copper to non-copper ratio from the previous plot. Figure 9 presents minimum cost and optimum field as functions of copper to non-copper ratio. Changing of the copper to non-copper ratio from 0.85 (short models) to 1.2 (necessary for the quench protection of a long magnet) increases the minimum collider cost by 2 % that is a fairly small but necessary price of a safe machine operation.

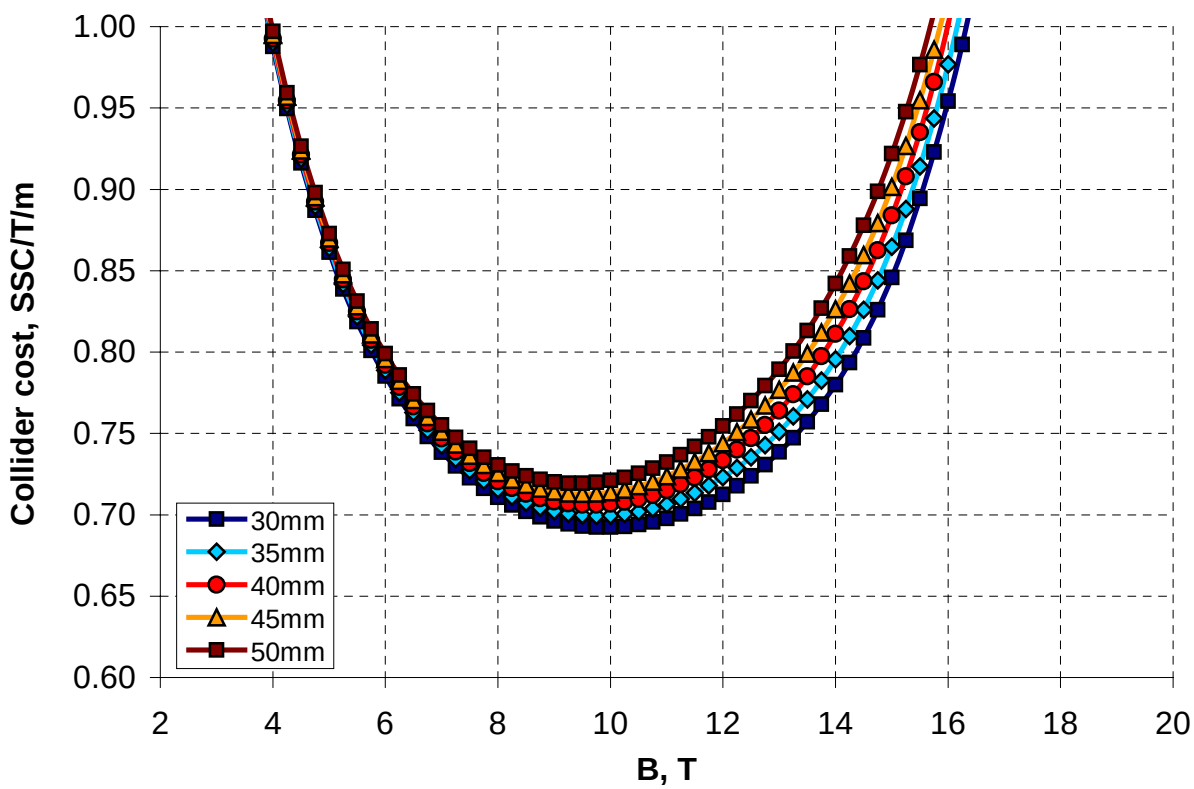

Figure 5. Collider cost as a function of field in SSC units for different coil apertures.

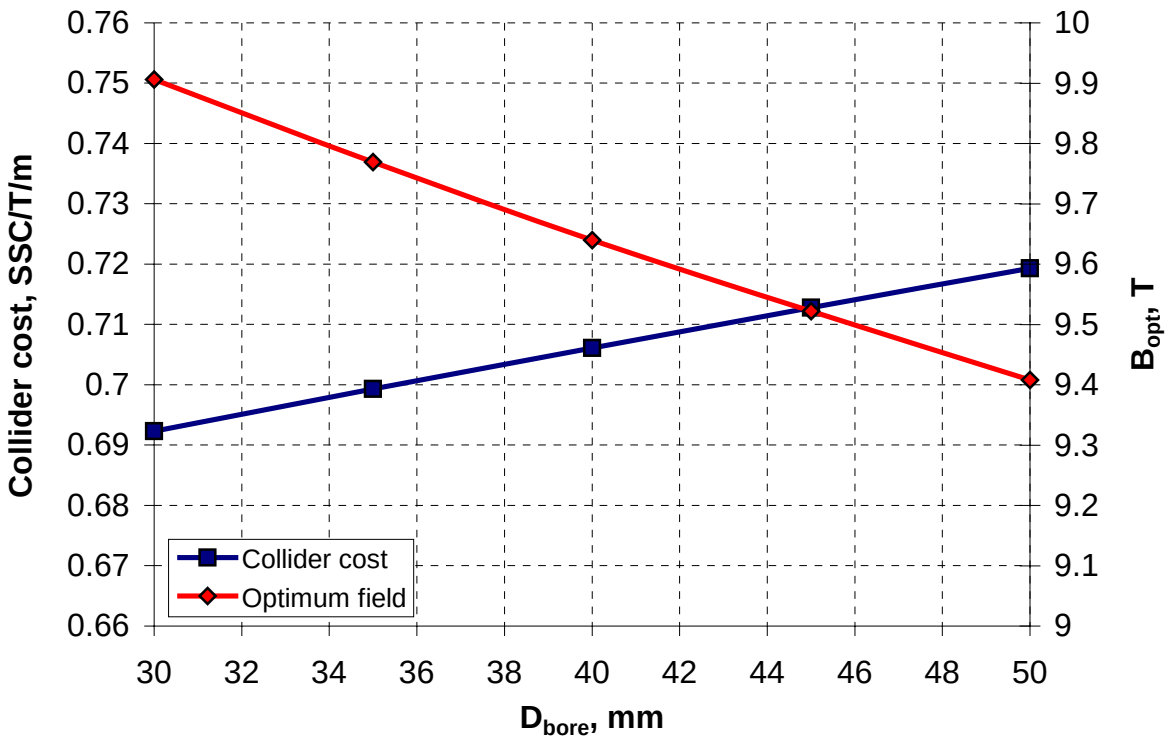

Figure 6. Minimum collider cost and optimum field as functions of bore diameter.

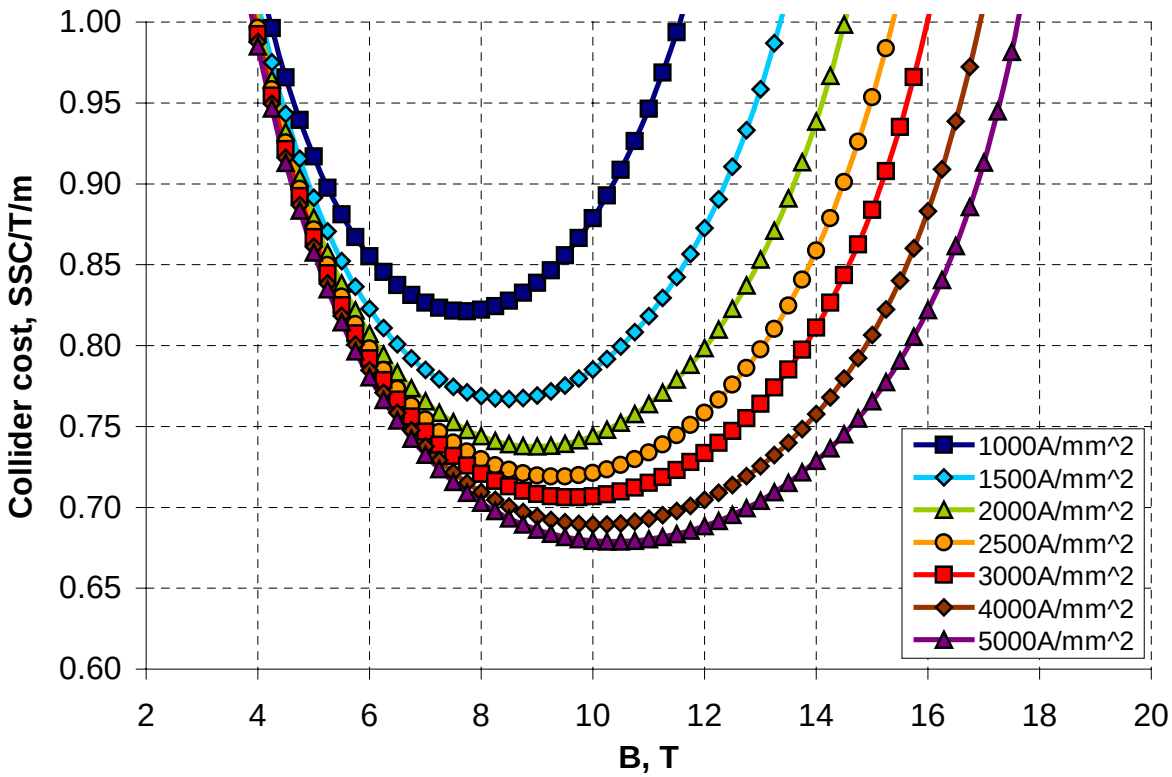

Figure 7. Collider cost as a function of field in SSC units for different critical current densities.

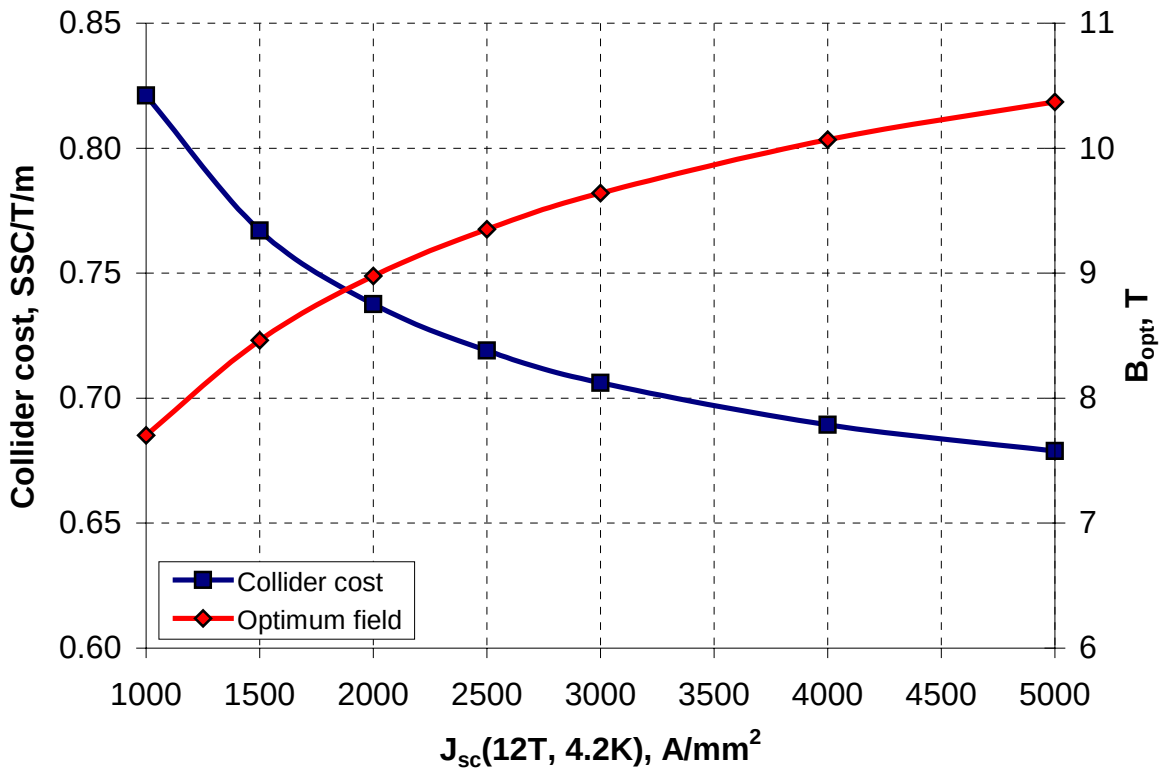

Figure 8. Minimum collider cost and optimum field as functions of critical current density.

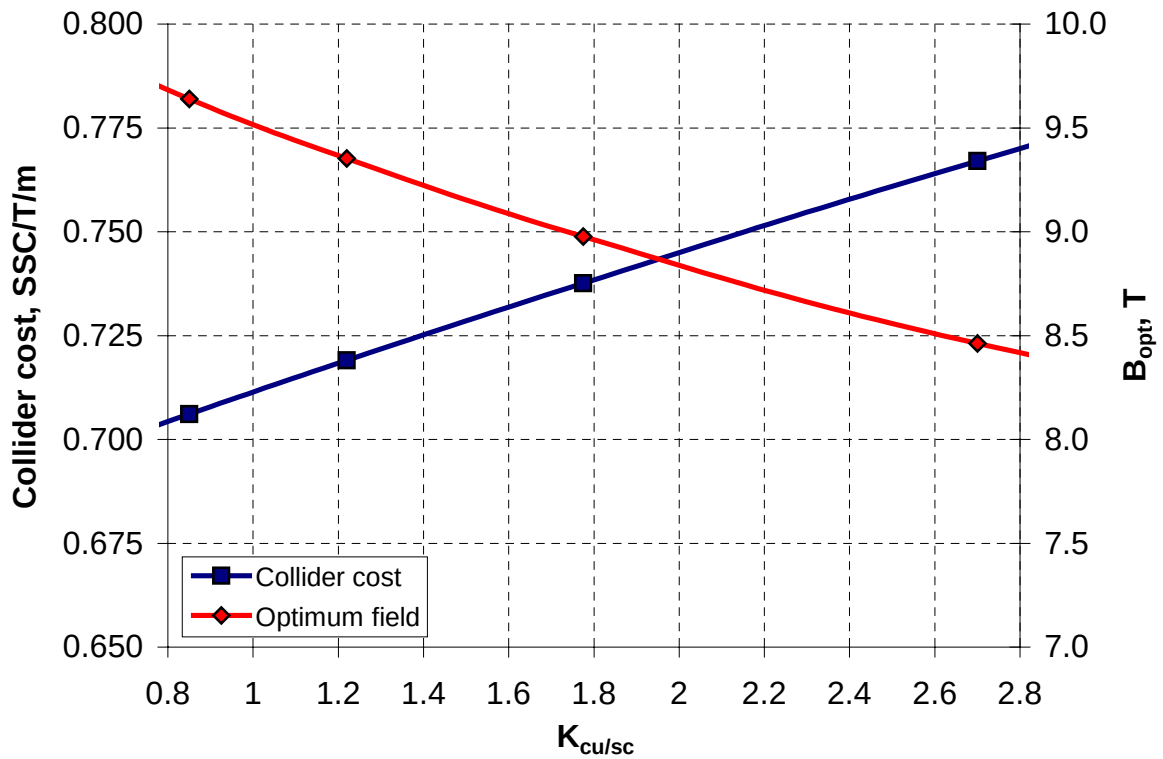

Figure 9. Minimum collider cost and optimum field as functions of copper to non-copper ratio.

5. Economical justification of a Nb_3Sn collider

In order for a collider based on Nb_3Sn superconductor to be economically effective, its cost should be less than that of a NbTi based collider. The model considered in previous paragraphs does not take into account difference in cost between NbTi and Nb_3Sn superconductors. It can be easily accomplished by adding corresponding term in (2.4):

$$C'_{mag}(R_{bore}, B) \sim S_{coil}(R_{bore}, B) K_{coil} K_{Nb_3Sn/NbTi} + R_{bore}{}^2 B^2 K_{cm} + R_{bore} B K_{cr},$$

where $K_{Nb3Sn/NbTi}$ is the ratio of price per unit volume between Nb_3Sn and NbTi superconductors. Iteratively repeating all the necessary steps one can find the price ratio that renders cost of Nb_3Sn collider to be equal to NbTi collider. This number is 4.7 for the Nb_3Sn collider with 40-mm bore magnets and critical current density of 3000 A/mm^2 at 12 T and 4.2 K. Figure 10 shows cost distribution for the corresponding NbTi and Nb_3Sn colliders. The optimum field for the NbTi collider is 6.5 T; for the Nb_3Sn collider with the price ratio of 4.7 is 7.5 T and for the Nb_3Sn collider with the price ratio of 1.0 is 10 T.

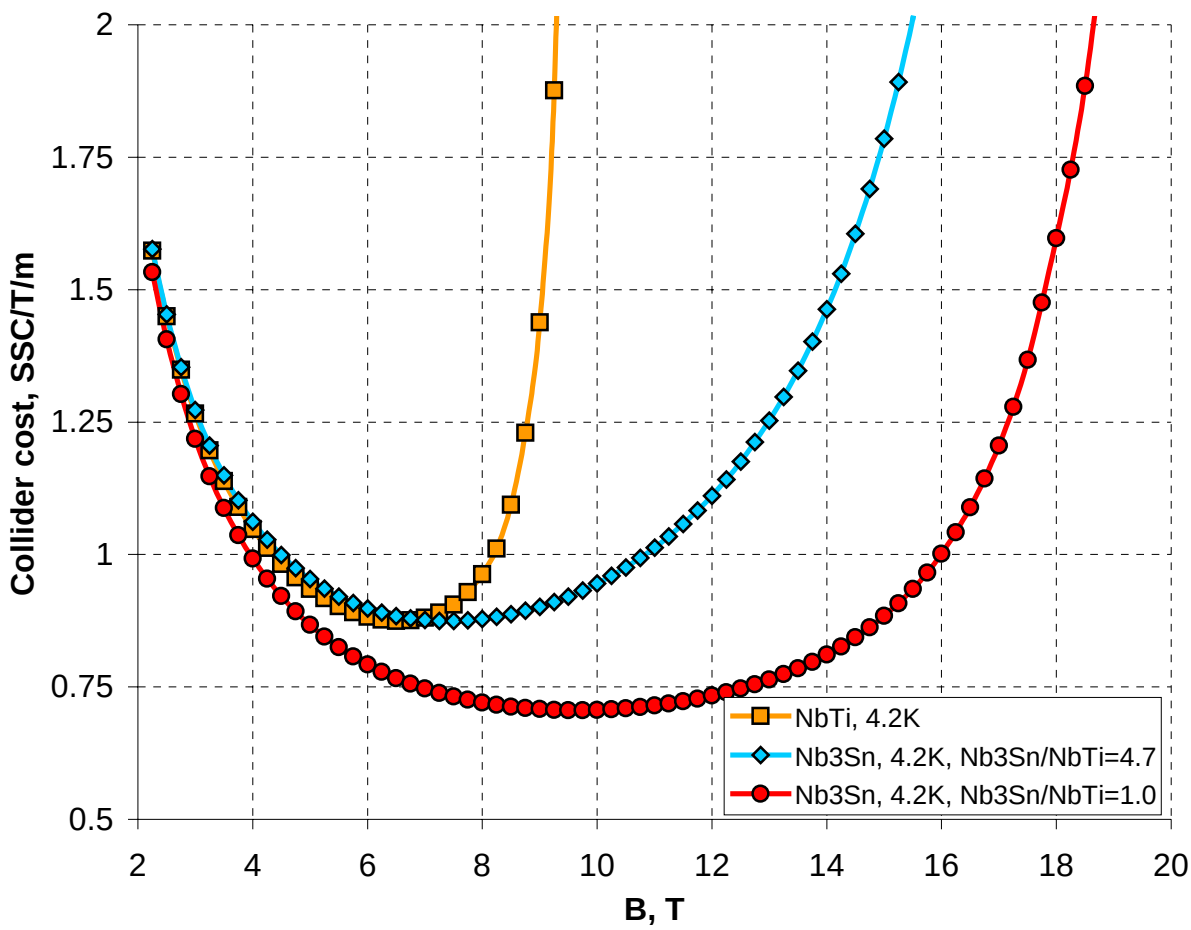

Figure 10. Collider cost as a function of field in SSC units.

Conclusion

The considered model based on reasonable assumptions allows cost comparison between colliders with different high field magnet parameters. Comparison between SSC, LHC and VLHC colliders shows consequent growth of the optimum operating field and reduction of the machine cost per T·m. Thus fully equipped tunnel of VLHC with the parameters justified during the design study [4] and the center-mass energy of 175 TeV would cost 3.1 times the SSC (40 TeV), when the same energy SSC would cost 1.4 times more under assumption of equal prices for Nb_3Sn and NbTi. Minimum on the cost curve, corresponding to the optimum field for VLHC is ~10 T, which is essentially smaller than fields practically achievable with modern Nb_3Sn conductors. Shallowness of the minimum, in fact, allows to define the optimum field range of 8-11 T. However, contribution of the synchrotron radiation (not included in the model) would cut the optimum range at the high field side, presumably to 8-10 T.

Analyzed influence of the magnet design parameters to the machine cost lets to conclude:

- Decreasing of the magnet aperture has a fairly weak effect on the machine cost. Taking into account cost contribution of the beam screen, cryogenics and magnet alignment, the optimum aperture is unlikely to be smaller than 40 mm. In fact, it may be even larger, especially for more than 10 T field magnets, where synchrotron radiation makes a significant cost contribution.
- Increasing of the critical current density in superconductor from 1000 A/mm^2 to 3000 A/mm^2 makes a noticeable machine cost reduction (16 %). Further increasing of the critical current density, however, has relatively small effect and may not be economically justified at all, due to necessity of significant investments in superconducting technology. Taking into account cabling and other types of critical current degradations, one would define the wanted critical current density in superconductor at 3500 A/mm^2.
- Variation of the copper to non-copper ratio within reasonable limits has a weak effect on the machine cost. Thus changing of the copper to non-copper ratio from 0.85 to 1.2, necessary for the quench protection of a long (>15 m) magnet, increases the collider cost by 2 % that seems to be unavoidable price of safe operation, unless a sophisticated quench protection system is developed.

Economical justification of a Nb_3Sn collider shows that the price of Nb_3Sn conductor may be as large as 4.7 times the price of NbTi for the collider to be economically effective. This price difference is virtually achieved for small quantities of Nb_3Sn superconductor and may be reduced even more after assessment of a large machine.

Further reduction of the collider cost per T·m is possible during R&D program. Using of high field magnets with “warm” iron yoke [6], for instance, allows reduction of the cryostat size by factor of ~ 2, while keeping other parameters uniform. Thus, depending on the design of the coil support structure, the cold mass cost can be reduced by factor of 3-4 and the cryostat (“warm” yoke) cost by at least factor of 2. Other improvements, leading to reduction of the labor part during coil production and increasing of a single magnet length by using of coils with minimum number of turns [3] are also beneficial.

References

1. J. McDonald, E. Barzi, A model for J_c in granular A-15 superconductors, IEEE Transactions on Applied Superconductivity, Vol. 11, No. 1, March 2001.
2. E. Willen, Superconducting magnets, INFN Eloisatron Project 34th Workshop, Erice, Sicily, November 4-13, 1996.
3. V.V. Kashikhin, A.V. Zlobin, Single-Layer High Field Dipole Magnets, PAC2001, Chicago, June 2001.
4. P.J. Limon, et. al., Design Study for a Staged Very Large Hadron Collider, Fermilab-TM-2149, June 2001.
5. P.J. Limon, The Study of a Staged-Energy VLHC at Fermilab, Accelerator physics and technology seminar, Fermilab, May 2001.
6. V.V. Kashikhin, A.V. Zlobin, Magnetic designs of 2-in-1 Nb_3Sn dipole magnets for VLHC, IEEE Transactions on Applied Superconductivity, Vol. 11, No. 1, 2176, March 2001.